Granular Matter
DOI 10.1007/s10035-015-0565-1

ORIGINAL PAPER

Stiffness evolution of granular layers and the origin of repetitive, slow, stick-slip frictional sliding

John Leeman[1] · Marco Maria Scuderi[1] · Chris Marone[1] · Demian Saffer[1]

Received: 23 July 2014

Abstract We demonstrate the frictional behaviors of steady state sliding, stick-slip, and repetitive, slow stick-slip sliding through a carefully-designed suite of laboratory experiments focused on exploring the role of loading system stiffness in controlling the frictional response to shear. We performed tests on sheared layers of baking flour, with three configurations of loading blocks made of steel and cast acrylic to achieve different stiffnesses. Slide-hold-slide and velocity step tests were conducted and analyzed in a rate-and-state friction framework. With compliant loading blocks, the material exhibits unstable stick-slip behavior with slow-slip events of duration up to 20 s. Slow-slip has been difficult to achieve in the lab and has only been observed for a narrow variety of boundary conditions and materials. Our results suggest that this behavior is strongly controlled by the stiffness of the system, the strain history of the sample, and shear fabric evolution. We describe a new suite of automated tools that greatly improve friction analysis and provide insight to the underlying mechanisms of slow stick-slip. We demonstrate that layer stiffness evolves with shear strain and modifies the mechanical behavior of stick-slip sliding. Our work suggests that slow earthquakes in tectonic fault zones may be linked to shear fabric development and associated changes in local stiffness, likely in combination with variations in frictional constitutive properties and effective stress.

✉ John Leeman
jleeman@psu.edu

1 The Pennsylvania State University, 522 Deike Building, University Park, PA, USA

Keywords Slow slip · Stick slip · Frictional stick slip · Critical stiffness · Rate and state friction

1 Introduction

Laboratory friction experiments are one common approach used to gain insight into earthquake physics. In these studies, powdered material is often used as an analog for the gouge that is a typical wear product within large-displacement tectonic fault zones. Frictional stick-slip behavior is the laboratory analog of the earthquake cycle [6]. Strain energy is stored in the gouge and surrounding materials as the system is elastically loaded. This energy is released when the stress on the fault reaches the yield strength, causing failure and movement. In typical laboratory manifestations of this behavior, the stick-slip events occur repeatedly and with characteristic time scales that are dictated by propagation of elastic waves through the sample. The magnitude and nature of the resulting stress drop is determined by the boundary conditions and material properties. There are relatively few laboratory materials that exhibit regular and reproducible stick-slip behavior. In most cases, experiments conducted under geophysical stresses contain only one or two stick slip events before the experiment is terminal. In experiments where multiple, highly reproducible stick slip events are needed, glass beads have become a common testing material. Soda-lime glass is a well characterized and homogeneous material that exhibits repetitive stick-slip and has been well studied [1,11,20,25,26].

Although stick-slip is generally considered an analog for earthquakes [7,18] in the framework of stable or unstable sliding, it has recently become evident that there is a spectrum of fault slip behaviors [32]. The discovery of slow earthquakes and non-volcanic tremor [5,14,16,30] has raised

Published online: 30 May 2015

questions about the link between fault zone frictional properties, in situ conditions, and the underlying mechanisms of slow-slip [19].

The rate and state frictional model provides a convenient framework in which to examine the frictional response of materials and characterize their second order frictional characteristics that are thought to control the stability of sliding [6,7,12,27]. The rate and state equation (Eq. 1) describes friction (μ) in terms of a direct effect (a), an evolution effect (b), a state variable (θ), and the velocity of both the slider (V) and load point or reference velocity (V_0). The evolution of the state variable can be described by various relations [27]. Here, we consider the Dieterich (slowness) relation (Eq. 2) as it provides a scheme to interpret time dependent healing of materials, although we note that recent works favor the Ruina (slip) state evolution law [3,29]. To describe more complex frictional behavior, a third term is often appended to Eq. (1) adding terms b_2, D_{c2}, and θ_2.

$$\mu = a\ln\left(\frac{V}{V_0}\right) + b\ln\left(\frac{V_0\theta}{D_c}\right) + b_2\ln\left(\frac{V_0\theta_2}{D_{c2}}\right) \tag{1}$$

$$\frac{\mathrm{d}\theta}{\mathrm{d}t} = 1 - \frac{V\theta}{D_c} \tag{2}$$

Materials may slide in a stable manner or fail in a stick-slip fashion. The transition between stable sliding and stick-slip is generally viewed as a Hopf bifurcation that can be thought of as occurring at a critical stiffness (k_c), defined in Eq. (3) for quasi-static motion [12,35]. For values of stiffness greater than k_c, the system is stable. When k approaches and falls below k_c, the system undergoes damped oscillations and then enters an unstable regime that corresponds to stick-slip behavior. From Eq. (3), it is clear that velocity strengthening materials ($a - b > 0$) should slide stably, because the critical stiffness becomes negative. They therefore: (1) are unlikely to nucleate large earthquakes; and (2) should arrest rupture that propagates into them. Velocity weakening materials ($a - b < 0$) may undergo stable sliding or stick-slip based on the stiffness of the system in relation to the effective normal stress and friction parameters, expressed by a critical stiffness. The idea of there being two modes of frictional failure (stable sliding and stick-slip) is a generalization of the spectrum of slip behaviors that occurs in the transition between the two [35].

$$k_c = \frac{b-a}{D_c} \tag{3}$$

For materials that exhibit stable sliding behavior, we can interrogate frictional parameters by imposing velocity steps or conducting slide-hold-slide tests (Fig. 1). During velocity step tests, the load point velocity is instantaneously changed from one velocity to another and the frictional response of the

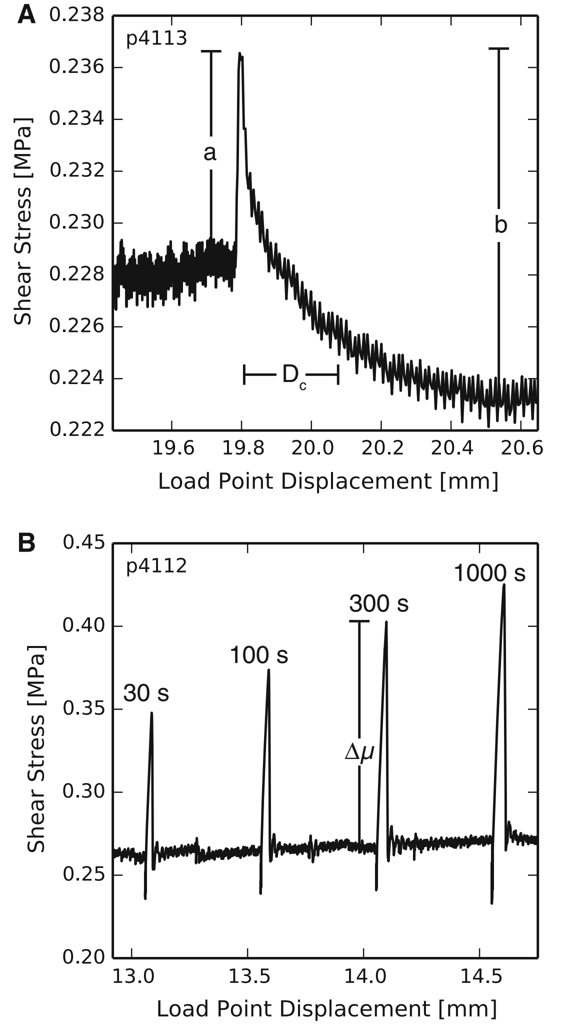

Fig. 1 Experimental data showing examples of tests used to measure rate-and-state frictional parameters. **a** Velocity step test in which loading velocity is changed from 150 to 500 µm/s. Note transient evolution of friction followed by attainment of a new steady-state. **b** Results for four slide-hold-slide tests in which shearing velocity is set to zero for a period (the hold) before re-shearing, showing holds of 30, 100, 300, and 1000 s. Frictional healing (μ) increases with the logarithm of hold time

material recorded. During slide-hold-slide tests, the sample is sheared until friction reaches steady-state (μ_{ss}), then shearing is stopped for a prescribed amount of time. After the hold time has elapsed, shearing begins again at a constant shearing rate and the frictional healing ($\Delta\mu$) is measured as the difference between the peak re-load friction (μ_{peak}) and the initial steady-state value [27]. Healing can be summarized by the term β, describing a line fit to hold-time (t_h) and frictional healing($\Delta\mu$) data on a natural log-linear axis (Eq. 4).

$$\beta = \frac{\Delta\mu}{\ln(t_h)} + c \tag{4}$$

The purpose of this paper is to describe work on a novel friction system designed to improve understanding of slow, stick-slip frictional failure. We measure the frictional behavior of sheared layers of baking flour and characterize slip events in terms of stress drop, slip duration, and the loading stiffness in order to explore the relationship between macroscopically observed slip behavior, stiffness, and frictional properties. We vary the stiffness of the loading system and observe changes in frictional failure behavior.

As in most shearing experiments, there are likely deformation and fracture processes occurring at the grain-scale, but these processes do not detract from the goal of showing failure mode behavior with stiffness changes. While flour is a very compliant material, certainly more compliant than the loading system, energy can be stored by the loading system while the fault zone is 'locked' and elastic strain energy accumulated in the loading blocks and load frame. Any air trapped in the granular layer is inconsequential as the low viscosity air can quickly escape as evidenced by our initial layer consolidation. Any remaining air is sufficiently compressible to produce negligible pressurization effects.

2 Methods

2.1 Experimental configuration

In our experiments, we sheared gouge layers in a double direct shear configuration using a biaxial deformation apparatus with a servo-hydraulic control system [11,20]. In this configuration, two granular layers are sheared between three roughened forcing blocks (Fig. 2). All experiments were conducted with Gold Medal brand all-purpose flour, enriched, bleached, and pre-sifted. The baking flour is highly compressible and is poly-disperse with grains ranging from about 10–200 µm in diameter (length) with a platy appearance (Fig. 3).

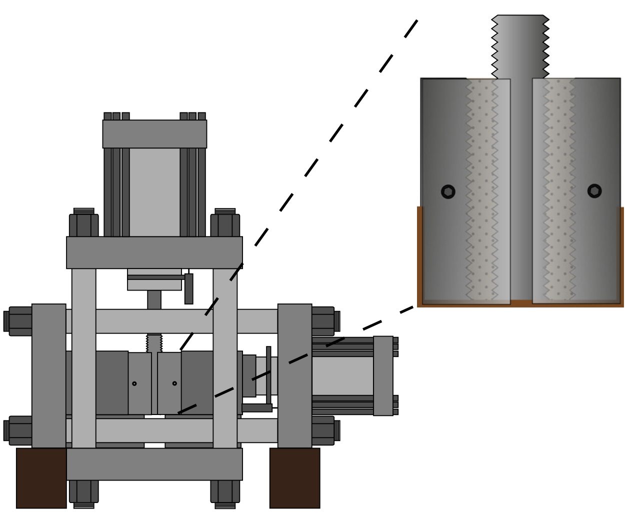

Fig. 2 The biaxial press with supporting and forcing blocks in place. Double-direct shear samples consist of three blocks: two side blocks and a center block. Gouge layers are between the forcing blocks and confined with side-shields and a rubber membrane (after [23])

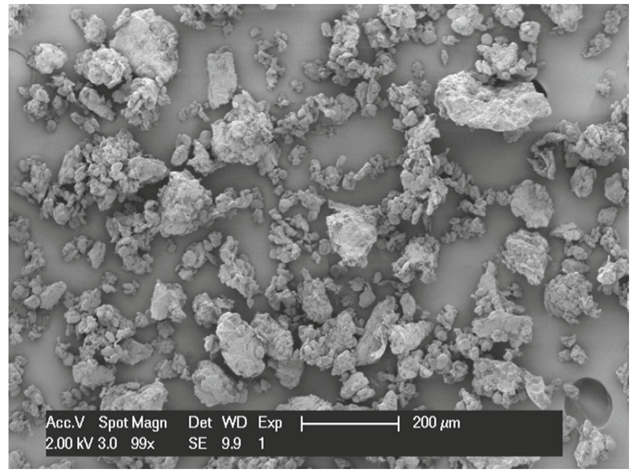

Fig. 3 A scanning electron micrograph of undeformed baking flour. Grain sizes are observed to vary in the 10–200 µm range. The material has a platy appearance reminiscent of clay and other phyllosilicate minerals

We measured force with strain gauge load cells placed in series with the loading rams and sample. Displacement was measured with direct current displacement transducers (DCDTs) between the ram nose and end platens of the hydraulic rams. Data were recorded using a 24-bit analog to digital converter. Data were collected at 10 kHz and averaged to the desired rate from 1 Hz to 10 kHz.

In order to achieve different loading system stiffnesses, three combinations of forcing blocks were used: (1) all acrylic blocks; (2) center acrylic with steel side blocks, and (3) all steel blocks. The forcing blocks were cut to size and machined with grooves (1 mm deep × 2 mm spacing on acrylic, 0.8 mm deep × 1 mm spacing on steel) perpendicular to the shearing direction to ensure that shear occurred within the layer and not at the layer boundary [1,22]. The nominal frictional contact area was 10 cm × 10 cm.

Layers were built by placing the side forcing blocks on a leveling jig and applying cellophane tape around the perimeter. Two layers of flour were confined in a three forcing block assembly with a rubber membrane at the bottom and side-shields on the boundaries to avoid lateral extrusion of the layer (Fig. 2). The top of the sample was unconfined.

In all experiments, samples were placed into the loading frame and a normal stress (σ_n) of 1 MPa was applied and maintained constant in load-feedback servo-control. The layers were sheared by controlling the position of the vertical ram in displacement feedback servo-control, which was driven at a constant displacement rate. The force required to shear at this rate was measured and converted to the shear stress acting on each layer of the double-direct shear arrangement.

In all experiments, a 'run-in' period was necessary to reach a stable sliding friction (Fig. 1). All tests were conducted at an initial load point velocity of 1 µm/s. In systems that exhibited unstable behavior, the run-in driving velocity was maintained for the duration of the test and the evolution of the slow-slip/stick-slip monitored. When stable sliding behavior was observed, a series of velocity steps and/or slide-hold-slide tests were performed to independently measure second-order frictional properties [27].

2.2 Data analysis

For each individual stick-slip event, we report stress drop, slip duration, recurrence time, and loading stiffness (Fig. 4). Note that for each event, a period of increasing shear load is observed initially followed by inelastic yielding and plastic strain accumulation during fully-mobilized frictional slip. The stress drop, duration, and recurrence time of each event provide information about frictional properties, including the rate of frictional healing. The linear-elastic portion of the stress-displacement curve (Fig. 4) is a measure of the system stiffness including testing machine, forcing blocks and sheared layers. This shear stiffness is a key parameter because it is the stiffness that will drive frictional instability if the value falls below the critical friction stiffness k_c dictated by Eq. (3).

With large numbers of slow-slip/stick-slip events it is necessary to automate the analysis procedure for both repeatability and efficiency. This is made difficult by electrical and mechanical noise as well as changes in recording rate during the course of the experiment. We address these challenges by developing an algorithm to pick the beginning and end of each slip event in a reliable and repeatable manner with as few user-defined free parameters as possible. After the picks are obtained, the mechanical quantities of interest must be extracted. Some values, such as changes in peak friction, are trivial to compute. However, loading stiffness is slightly more complicated, and requires determining where the load-displacement curve deviates from linearity. We address this problem by using a goodness-of-fit approach, detailed in "Appendix".

3 Results

We varied system stiffness by using a range of forcing blocks in the double direct shear assembly. Tests with all acrylic forcing blocks and with acrylic center/steel side block combinations produced slow slick-slip behavior, while tests with all steel blocks generally produced stable sliding behavior (Fig. 5). For the experiments with steel forcing blocks, frictional sliding was stable. Thus, once friction reached a steady state, we imposed velocity step tests to measure rate/state friction parameters. We note that in one experiment, at 5 µm/s, the steel block configuration exhibited slow-slip behavior, transitioning to stable sliding at higher velocities. During shear, extrusion and densification of the gouge material occurs [37], sometimes introducing complicating strain effects.

Slide-hold-slide tests were used to measure frictional healing. Healing tests conducted with steel forcing blocks indicate healing rates (β) of 0.015–0.018. These rates are

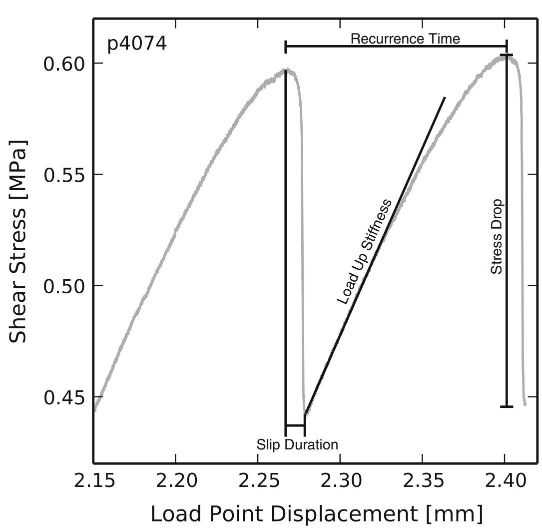

Fig. 4 Slow-slip and stick-slip events can be characterized by their slip duration, recurrence time, stress drop, and elastic loading stiffness. These quantities can be used to quantify the effective system stiffness and frictional properties including the rate of restrengthening (healing)

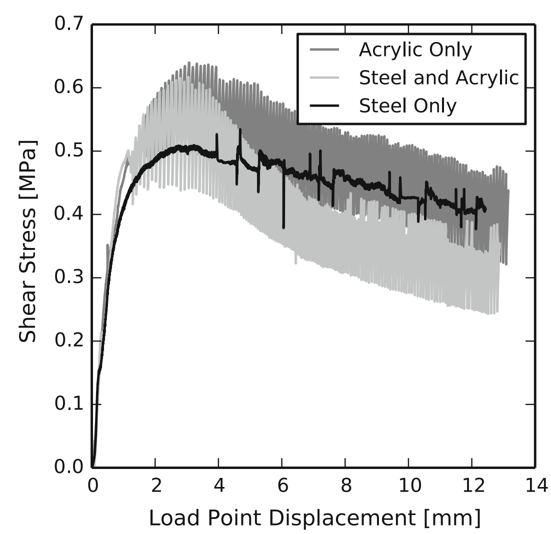

Fig. 5 Data for three experiments with different forcing blocks and effective system stiffnesses. The acrylic only and steel-acrylic experiments exhibited slow stick-slip behavior, while steel forcing blocks produced only stable sliding

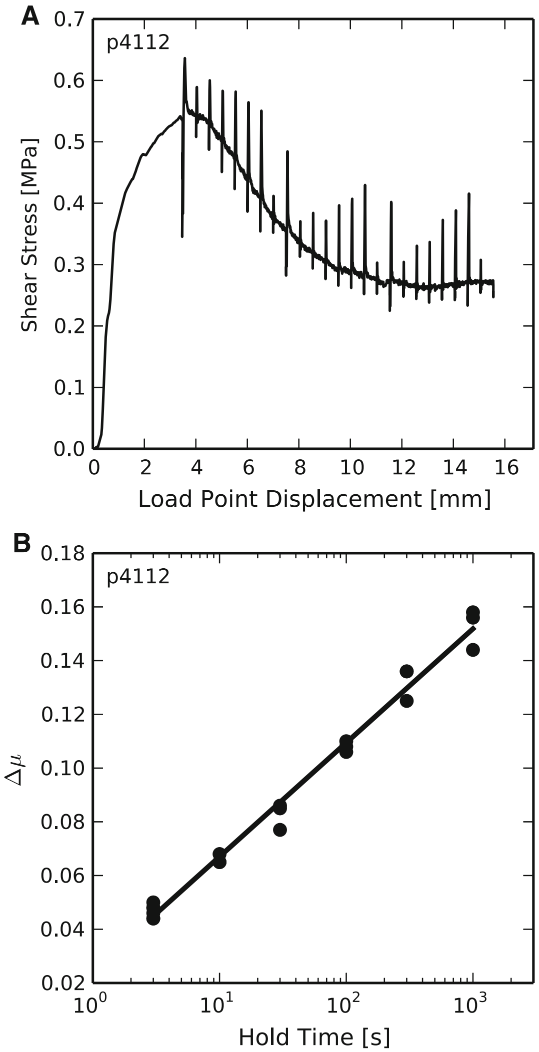

Fig. 6 **a** Friction data during slide-hold-slide tests over an entire experiment with steel forcing blocks. Note initial load-up: there is a region of peak strength followed by weakening and the attainment of steady-state strength after shear of ~10 mm. This test included three sets of holds lasting from 3 to 1000 s. **b** Friction parameter $\Delta\mu$ versus the log of hold time for the slide-hold-slide tests shown in (**a**). Healing exhibits log-linear behavior, independent of net shear displacement

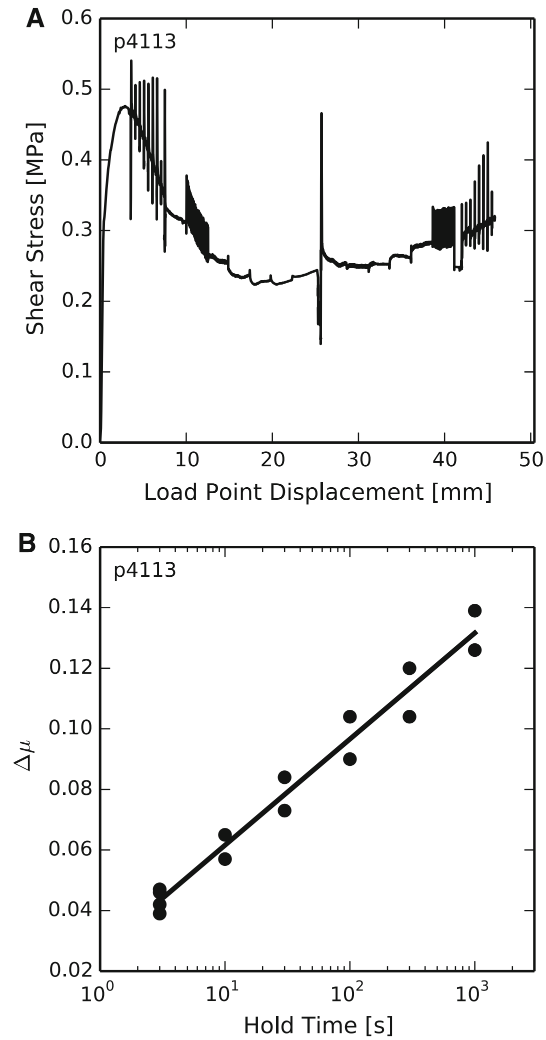

Fig. 7 **a** Friction data for experiment p4113 with steel loading blocks, and **b** healing determined from slide-hold-slide tests. The sample exhibited limited stick-slip/slow-slip behavior, but only at a load point velocity of 5 µm/s. Frictional instability appears as a wide band of noise at the scale shown, around 10 and 40 mm load point displacement. Holds ranged from 3 to 1000 s and velocity steps from 5 to 1500 µm/s

consistent with rates obtained on geological materials of several percent [4,9,10,21,27]. We imposed three sets of slide-hold-slide tests at successively higher shear displacements and found no correlation of the healing rate with shear strain, in contrast to previous results [36]. We note however that those studies used granular silicate minerals at higher applied stresses, and thus higher rates of granular comminution. Also, the maximum shear strain in our experiments were less than those in other studies (Fig. 6). We conducted slide-hold-slide tests before and after velocity step tests to determine any variation with shear strain. Even after shear displacement of nearly 5 cm, no significant change in healing rate was observed (Fig. 7). All of our data exhibit a log-linear relationship between healing and hold time.

Velocity step tests were conducted with both up-steps and down-steps in the range: 5, 15, 50, 150, 500, 1500 µm/s in the steel forcing block configuration. At 5 µm/s the system was unstable, but then exhibited stable behavior at higher velocities. Model fits of selected velocity steps are shown in Fig. 8. These data show velocity weakening frictional behavior with $(a - b)$ values of ~ -0.01 and friction evolution shows a clear two state variable behavior. Best fit parameters are summarized in Table 1.

In most friction studies, the system stiffness is taken from a linear portion of the loading curve prior to the sample yielding and attainment of fully mobilized, steady-state frictional sliding. Moreover, this stiffness is generally thought of as the stiffness of the system for the entire experiment. The values

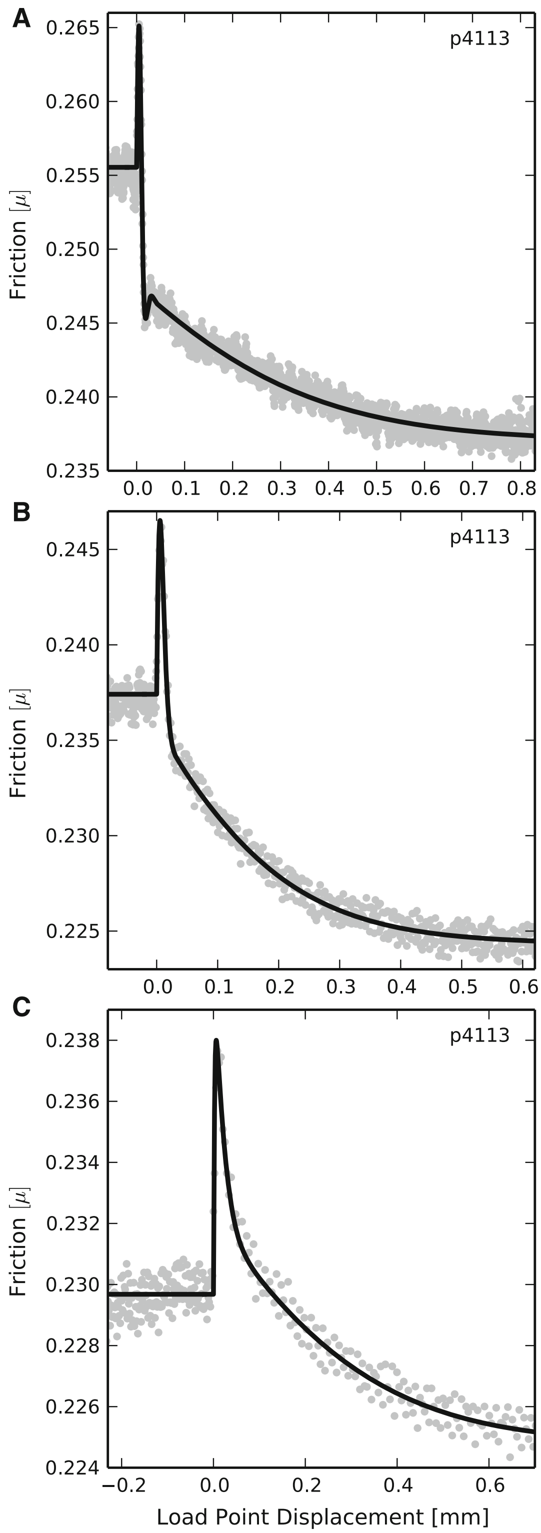

Fig. 8 Velocity steps in an all steel forcing block configuration can only be fit by a two state variable model. **a** 15–50 μm/s, **b** 50–150 μm/s, **c** 150–500 μm/s

in Table 2 represent the load up stiffness determined via this traditional approach. Load up stiffness values are obtained by fitting a line to the load up curves during experimental run-in. Values for all-steel and steel/acrylic are relatively similar, but the all-acrylic forcing system is about one-third less stiff than the steel system.

We applied our automated picking algorithm for experiments with unstable behavior in acrylic and acrylic/steel blocks. The steel system displayed dominantly stable sliding and could not be interrogated for stiffness with this method. The experiment with all acrylic forcing blocks showed a stress drop pattern that increased to a relatively steady value of 0.014 MPa (Fig. 9). Slip durations began at ∼20 s, then decreased to ∼5 s. Shear loading stiffness increased with shear strain from ∼0.001 to ∼0.002 MPa/μm with shear strain until frictional steady state behavior was reached, and then remained stable for the duration of the experiment. Experiments with the steel/acrylic combination (Fig. 10) show similar stiffness evolution, but the slip durations are much more scattered compared to the all acrylic configuration. These data show the same initial increase in the stress drop, but then decrease to almost their initial states. Finally, there is a second 'family' of slip events that appear around event 80 with much larger stress drops (Fig. 11). These events exhibit the same minimum shear stress, but reach a higher stress before failure. There is also a notable partial failure observed at the nominal shear strength.

4 Discussion

Our data show that stiffness evolves systematically as a function of shear strain and that stick-slip friction events reflect this evolution. Load point velocity also plays an important role in the transition from stable to unstable sliding.

It has long been known that loading stiffness plays an important role in frictional sliding [6,17], and since its introduction in the 1980's, rate and state friction theory has provided an approach to quantifying the interplay between elastic stiffness and friction constitutive behavior (Eq. 3) [34]. Previous works show that the critical friction distance (D_c) decreases with shear strain [28]. However, the evolution of fault zone stiffness with shear strain has not been similarly explored. Our results show that stiffness increases by nearly a factor of two during initial shearing, up to shear strains of ∼3. These changes are likely a function of densification, shear localization, and fabric development as elongated particles align and shear begins to attain its steady state behavior. The fact that characteristics of stick-slip events, such as stress drop and slip duration, evolve over this same range, suggests that both changes in frictional properties and elastic stiffness are important in controlling the mode of slip on faults.

Rate and state friction predicts increased event durations and decreased stress drops with increased effective stiffness, as the system transitions to stable behavior [2]. Our data comparing the different stiffnesses from the three forcing block

Table 1 Two state variable parameters obtained from friction data inversion with all steel forcing blocks (p4113)

V_0	V	a	b_1	D_{c_1}	b_2	D_{c_2}	$a-b$
15	50	0.0120	0.0185	5.351	0.0088	207.912	−0.0154
50	150	0.0110	0.0125	7.448	0.0105	127.545	−0.0119
150	500	0.0077	0.0056	15.432	0.0061	199.407	−0.0041

Table 2 Load up stiffnesses during run-in for different forcing block configurations

Experiment	Blocks	Layer thickness (mm)	Temperature (C)	Relative humidity (%)	Loading stiffness (MPa/μm)
p3916	Acrylic	7	23.5	22	0.000630
p3918	Acrylic	7	23.1	22	0.000917
p3919	Acrylic	7	24.2	23.9	0.000762
p3920	Acrylic	7	24.4	25	0.000871
p3917	Steel/acrylic	7	22	21.9	0.001002
p4074	Steel/acrylic	8	23.1	38.8	0.001142
p4073	Steel	8	23.4	28.4	0.001426
p4112	Steel	8	24.3	55.5	0.001184
p4113	Steel	8	24.3	56.1	0.001070

Note that the steel/acrylic combination is much closer to the stiffness of all steel blocks than that of all acrylic blocks

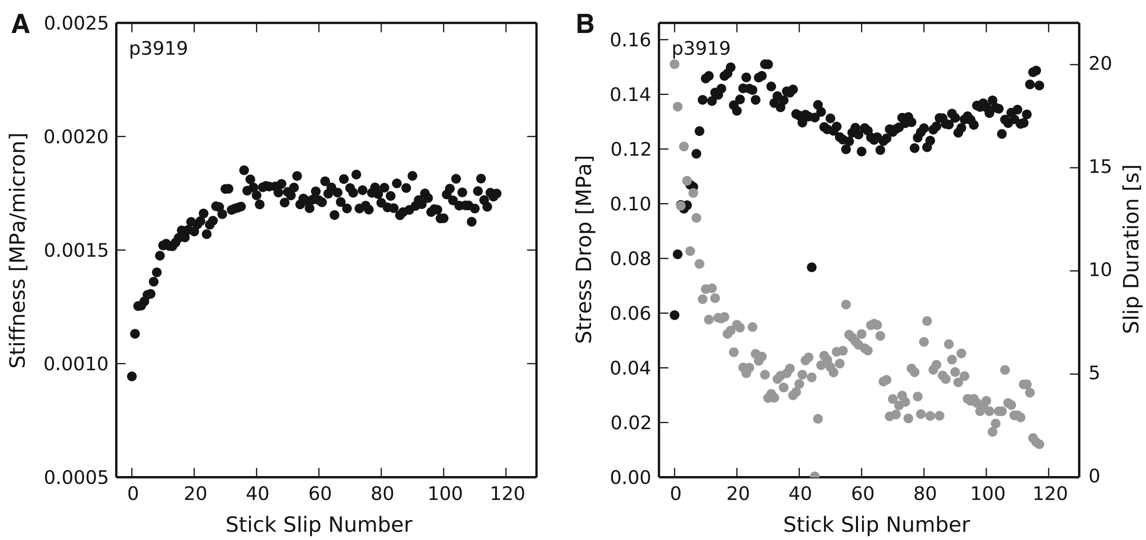

Fig. 9 **a** Stiffness and **b** stress drop and slip duration for events in experiments with all acrylic forcing blocks. Stiffness increases on the rise to steady state by a factor of nearly two and remains remarkably constant. Stress drops rapidly increase by a factor of two over the first 20 events before reaching a steady state. Slip duration begins at nearly 25 s, then rapidly decreases to around 5 s

configurations used seems to verify this prediction (Fig. 12). However, during each experiment, we observe an increase in stiffness with shear strain that coincides with increased stress drop and reduced slip event duration (Figs. 9,10). This suggests a more complex interplay between the evolution of fabric development, frictional constitutive properties, and system stiffness with shear strain that produces changes in material behavior. Coupling of the stored elastic energy is also believed to influence strain accumulation and release. Because the entire center forcing block acts as a spring (i.e. stores elastic strain), a simple 1-D spring-slider model is overly simplified in the context of our experiments. Accounting for the 2-D geometry and heterogeneity of the elastic loading system that includes both forcing blocks and the gouge layer itself is more realistic. This more complicated elastic coupling would influence the nature of strain accumulation, and the rate at which it is released during failure. The stiffness of the portions of the system where elastic strain energy is stored is most important, as the unloading stiffness of those materials will dictate the rate at which energy can be

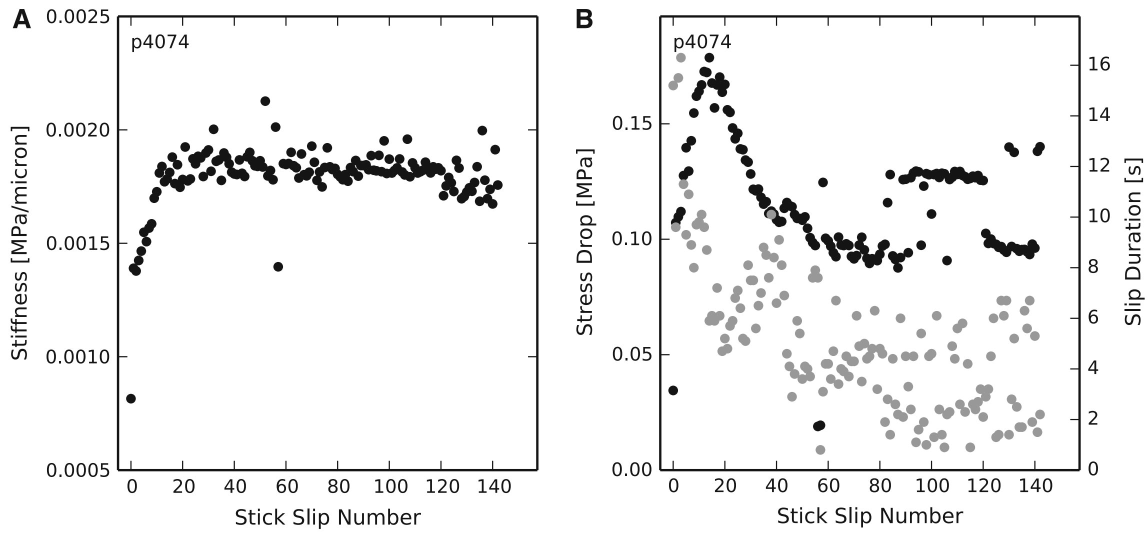

Fig. 10 **a** Stiffness and **b** stress drop and slip duration for events in the steel/acrylic forcing block system. Stiffness follows a similar trend to the all-acrylic experiment, but exhibits a smaller increase with strain. Stress drop increases rapidly, but then returns and maintains its initial level until a second family of events occurs around events 80–120. Slip duration begins faster than for the all-acrylic blocks and stays lower with more scatter

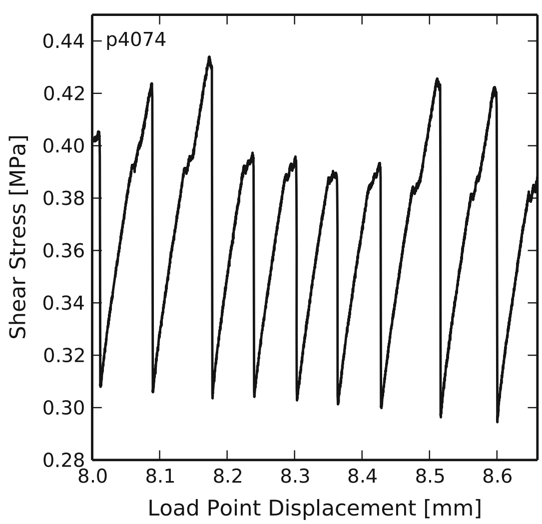

Fig. 11 Two groups of stick-slip events are evident after sufficient shearing in the steel/acrylic system. At the expected shear failure point there are several small failures, but the layer recovers and continues to load to a higher stress before failure

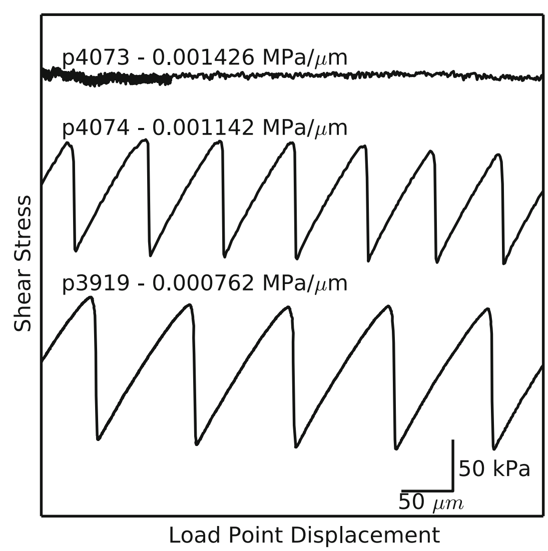

Fig. 12 Response of the system with various effective stiffnesses. The stability boundary is crossed between the steel and steel/acrylic system. Stiffnesses shown are the initial load up stiffnesses of the sample. All data are from the same displacement range, but have been offset in shear stress for clarity

released to the system during dynamic failure and therefore dictate the failure mode. While the gouge is itself storing some strain energy, we believe that most energy is being stored in the forcing blocks while the fault zone is locked, hence why the block stiffness exhibits such a strong control on failure mode.

Our data suggest that as strain localizes within the sheared layer, the stiffness of the gouge layer increases, resulting in an overall stiffer elastic system. Strain is localized onto shear surfaces oblique to the layer, such as R1 (cross cutting shear surfaces inclined approximately 30° to the shear direction), B (bounday parallel shears near the forcing block surface), and y (shear parallel surfaces completely contained within the layer) planes [24,27]. The transition of slip behavior from steady-state sliding to stick-slip (Fig. 12) is apparent and follows results obtained by Baumberger and Berthoud [2]. By using compliant blocks that have the capability to store energy where the gouge is interacting with the surface roughness (i.e. rather than steel forcing blocks with a spring in series to modulate stiffness [19]), we believe that our approach is most analogous to natural fault zones, in which the gouge is coupled to adjacent wall rocks that store strain energy between slip events.

Another curious aspect of these experiments is the unstable behavior observed in steel blocks, but only at low velocity in p4113 (the least stiff of the steel experiments). Even in acrylic blocks, the system would only stick slip at velocities below 100 μm/s. This is consistent with previous observations of the transition from stick-slip to stable sliding [13]. In our experiments, it is possible that healing cannot occur fast enough to support repeated stick-slip behavior at higher velocities. Flour maintains its strong velocity weakening behavior at velocities up to 1500 μm/s, suggesting that stiffness and/or velocity dependent rate and state parameters are necessary to explain the velocity dependent behavior.

Stiffness relations used in arguments about stick slip and slow-slip events often cite critical rupture patch sizes by assuming an inverse relationship between effective stiffness and nucleation patch size [15]. While this argument is valid and physically required, it is likely equally important to consider that effective stiffness evolves during the transition from distributed to localized shear [29]. This combination of factors modifying stiffness likely leads to a more complex fault zone evolution than previously believed. Local variations in stiffness could modulate shear behavior and velocity during rupture propagation or even aid in stopping fast rupture. One possible indication of the local variability of stiffness is the two families of stick-slip events observed in the steel/acrylic case. This behavior is reminiscent of period-doubling in chaotic systems near a critical point. These smaller events could represent local heterogeneities which are too small to rupture the entire layer. It is also very likely that the 1-D stiffness coupling is inadequate to fully describe the system.

5 Conclusions

We show that repetitive, slow, stick-slip frictional sliding can occur in a sheared layer and that the transition from stable to unstable sliding can be affected by a change in system loading stiffness. While it is not a surprising revelation that stiffness is a factor in frictional slip behavior, the evolution of stiffness with strain that we observe points to a more complicated story. We suggest that stiffness evolves as shear fabric is developed in the layer with increasing shear displacement. This indicates that fault slip style, which is partly dictated by stiffness, may not depend solely on the inverse relation of loading system stiffness to sample dimension. In our system, it is possible that stiffness of the gouge evolves enough to cause a transition from stable sliding to slow-slip/stick-slip behavior. If our results apply to tectonic faults, they suggest that with progressively increasing net strain/offset, areas experiencing slow-slip events may evolve to an unstable slip condition with potential to host traditional seismic events. Our results were obtained for wheat flour, and it remains to be seen whether similar behavior occurs in geologic materials. We have found similar behavior in preliminary work on finely ground quartz. Further investigation is warranted to determine the range of conditions for which slow slip may occur and whether such behavior is possible for other types of elastic coupling. Work is also underway to measure strain energy stored in the system before, during, and after failure to attempt to quantify some of the possible explanations proposed in this work.

Acknowledgments We thank S. Swavely for help in the laboratory and Paul Johnson and Pierre-Yves Le Bas for helpful discussions. The manuscript was improved through comments of two anonymous reviewers. This work was supported by an IGPP Project funded through Los Alamos National lab and by NSF Awards EAR054570, EAR0746192, and OCE-0648331 to CM and NSF DGE1255832 to JL. Any opinions, findings, and conclusions or recommendations expressed in this material are those of the author(s) and do not necessarily reflect the views of the National Science Foundation. No animals were used during the course of this study.

6 Appendix: Algorithm description

We define stick-slip by a stress increase over some time interval and a sudden drop in stress, followed by another event. There are many techniques in the literature of ‘change point detection’ such as CUSUM [31], Student’s T test techniques [8], and wavelet methods [33]. These techniques are generally used for step detection and are not the ideal candidates for repetitive events such as repeating frictional slip. Picking based on derivatives is a more robust technique, and therefore we employ a first-derivative based approach. When the stress is at a peak or trough, the first derivative (with time or shear displacement) is zero by definition. We examine the derivative of shear stress for a sign change or zero crossing as it is unlikely that we will exactly capture the data points for which the derivative is zero to machine precision.

Taking the derivative of noisy, digital lab data can be challenging. In general, for an analytic function or data with no noise, we would approach the problem by using a forward, central, or backward difference approximation. These simplistic techniques work for well-behaved functions with no noise, but for lab data, a running average slope works better. Our method involves a user-defined window size over which a least-squares approach is used. This resulting running average slope technique is robust for noisy data.

To determine loading stiffness of each stick-slip event, we began with the derivative of the stress-displacement curve (Fig. 4). We then computed an array of signs for the complete data set. Sign change detection identifies the zero-crossings of the running average slope derivative. Pairs of zero crossings are evaluated for their associated stress drop, with anything below a user defined threshold discarded. This step is necessary to further filter noise and smaller failures. Using the zero crossing generally captures the true maximum and minimum of the data, but occasionally, due to smoothing of noise, may not capture the exact maximum or minimum. After observing the algorithm on many datasets, we found that max/min errors were always small and within the noise; therefore we did not implement a local search around the zero crossing.

The objective when determining the linear-elastic stiffness of each stick-slip is to fit a line to the displacement versus shear stress data, but only to the portion before inelastic deformation and creep begins. In the past this has been done by eye and resulted in limited estimates of stiffness for each experiment as well as inconsistency between picks. To automate this process, we calculate the correlation coefficient of the data (Eq. 5) for many data windows. The algorithm begins with the minimum shear stress for an event with n data, determined by the derivative technique, and calculates the correlation of three data points (the trough and the two following points). Next, the correlation is calculated for additional data points, up to $n_{\max}$. We assume that the deviation from linearity begins after the correlation is maximized. After we define the linear domain, a line is fit to that data segment using a least squares method. This process is repeated for each stick-slip/slow-slip event.

$$r_{xy} = \frac{\sum_{i=1}^{n} x_i y_i - \sum_{i=1}^{n} x_i \sum_{i=1}^{n} y_i}{\sqrt{n \sum_{i=1}^{n} x_i^2 - \left(\sum_{i=1}^{n} x_i\right)^2} \sqrt{n \sum_{i=1}^{n} y_i^2 - \left(\sum_{i=1}^{n} y_i\right)^2}}. \tag{5}$$

References

1. Anthony, J.L., Marone, C.: Influence of particle characteristics on granular friction. J. Geophys. Res. **110**(B8), B08,409 (2005)
2. Baumberger, T., Berthoud, P.: Physical analysis of the state- and rate-dependent friction law. II. Dynamic friction. Phys. Rev. B **60**(6), 3928–3939 (1999). doi:10.1103/physrevb.60.3928
3. Bayart, E., Rubin, A., Marone, C.: Evolution of fault friction following large velocity jumps. In: AGU Fall Meeting Abstracts, vol. 1, p. 0180 (2006)
4. Beeler, N., Tullis, T., Weeks, J.: The roles of time and displacement in the evolution effect in rock friction. Geophys. Res. Lett. **21**(18), 1987–1990 (1994)
5. Beroza, G.C., Ide, S.: Slow earthquakes and nonvolcanic tremor. Ann. Rev. Earth Planet. Sci. **39**(1), 271–296 (2011)
6. Brace, W.F., Byerlee, J.D.: Stick-slip as a mechanism for earthquakes. Science **153**(3739), 990–992 (1966). doi:10.1126/science.153.3739.990
7. Brace, W.F., Byerlee, J.D.: Mechanical instabilities observed in laboratory experiments on rocks. Eos Trans. AGU **50**(5), 400 (1969). doi:10.1029/eo050i005p00400-05
8. Buishand, T.A.: Some methods for testing the homogeneity of rainfall records. J. Hydrol. **58**(1), 11–27 (1982)
9. Dieterich, J.H.: Time-dependent friction in rocks. J. Geophys. Res. **77**(20), 3690–3697 (1972)
10. Dieterich, J.H.: Time-dependent friction and the mechanics of stick-slip. Pure Appl. Geophys. **116**(4–5), 790–806 (1978)
11. Frye, K.M., Marone, C.: Effect of humidity on granular friction at room temperature. J. Geophys. Res. **107**(B11), 2309 (2002)
12. Gu, J.C., Rice, J.R., Ruina, A.L., Tse, S.T.: Slip motion and stability of a single degree of freedom elastic system with rate and state dependent friction. J. Mech. Phys. Solids **32**(3), 167–196 (1984)
13. Heslot, F., Baumberger, T., Perrin, B., Caroli, B., Caroli, C.: Creep, stick-slip, and dry-friction dynamics: experiments and a heuristic model. Phys. Rev. E **49**(6), 4973 (1994)
14. Ide, S., Shelly, D.R., Beroza, G.C.: Mechanism of deep low frequency earthquakes: further evidence that deep non-volcanic tremor is generated by shear slip on the plate interface. Geophys. Res. Lett. **34**(3), L03,308 (2007)
15. Ikari, M.J., Marone, C., Saffer, D.M.: On the relation between fault strength and frictional stability. Geology **39**(1), 83–86 (2011). doi:10.1130/g31416.1
16. Ikari, M.J., Marone, C., Saffer, D.M., Kopf, A.J.: Slip weakening as a mechanism for slow earthquakes. Nat. Geosci. **6**(6), 468–472 (2013)
17. Jaeger, J.C.: Friction of rocks and stability of rock slopes. Géotechnique **21**(2), 97–134 (1971). doi:10.1680/geot.1971.21.2.97
18. Johnson, P.A., Ferdowsi, B., Kaproth, B.M., Scuderi, M., Griffa, M., Carmeliet, J., Guyer, R.A., Le Bas, P.Y., Trugman, D.T., Marone, C.: Acoustic emission and microslip precursors to stick-slip failure in sheared granular material. Geophys. Res. Lett. **40**(21), 5627–5631 (2013). doi:10.1002/2013gl057848
19. Kaproth, B.M., Marone, C.: Slow earthquakes, preseismic velocity changes, and the origin of slow frictional stick-slip. Science **341**(6151), 1229–1232 (2013)
20. Karner, S.L., Marone, C.: Effects of loading rate and normal stress on stress drop and stick-slip recurrence interval. Geophys. Monogr. Ser. **120**, 187–198 (2000)
21. Karner, S.L., Marone, C., Evans, B.: Laboratory study of fault healing and lithification in simulated fault gouge under hydrothermal conditions. Tectonophysics **277**(1), 41–55 (1997)
22. Knuth, M., Marone, C.: Friction of sheared granular layers: role of particle dimensionality, surface roughness, and material properties. Geochem. Geophys. Geosyst. **8**(3), Q03012 (2007). doi:10.1029/2006GC001327
23. Leeman, J.R., Scuderi, M.M., Marone, C., Saffer, D.M., Shinbrot, T.: On the origin and evolution of electrical signals during frictional stick slip in sheared granular material. J. Geophys. Res.: Solid Earth (2014). doi:10.1002/2013jb010793
24. Logan, J., Dengoz, C., Higgs, N., Wang, Z.: Fabrics of experimental fault zones: their development and relationship to mechanical behavior. Fault Mech. Transp. Prop. Rocks **51**, 33 (1992)
25. Mair, K., Abe, S.: Breaking up: comminution mechanisms in sheared simulated fault gouge. Pure Appl. Geophys. **168**(12), 2277–2288 (2011)
26. Mair, K., Frye, K.M., Marone, C.: Influence of grain characteristics on the friction of granular shear zones. J. Geophys. Res.: Solid Earth (1978–2012) **107**(B10), ECV 4-1–ECV 4-9 (2002)
27. Marone, C.: Laboratory-derived friction laws and their application to seismic faulting. Ann. Rev. Earth Planet. Sci. **26**(1), 643–696 (1998). doi:10.1146/annurev.earth.26.1.643
28. Marone, C., Kilgore, B.: Scaling of the critical slip distance for seismic faulting with shear strain in fault zones. Nature **362**(6421), 618–621 (1993). doi:10.1038/362618a0
29. Marone, C., Saffer, D.M.: The mechanics of frictional healing and slip instability during the seismic cycle. In: Gerald Schubert (ed.) Treatise on Geophysics, 2nd edn, pp. 111–138. Elsevier, Oxford (2015)
30. Obara, K.: Nonvolcanic deep tremor associated with subduction in southwest Japan. Science **296**(5573), 1679–1681 (2002)

31. Page, E.: Continuous inspection schemes. Biometrika **41**(1/2), 100–115 (1954)
32. Peng, Z., Gomberg, J.: An integrated perspective of the continuum between earthquakes and slow–slip phenomena. Nat. Geosci. **3**(9), 599–607 (2010)
33. Raimondo, M., Tajvidi, N.: A peaks over threshold model for change-point detection by wavelets. Stat. Sin. **14**(2), 395–412 (2004)
34. Rice, J.R.: Constitutive relations for fault slip and earthquake instabilities. Pure Appl. Geophys. **121**(3), 443–475 (1983)
35. Rice, J.R.: Gu, Jc: Earthquake aftereffects and triggered seismic phenomena. PAGEOPH **121**(2), 187–219 (1983). doi:10.1007/bf02590135
36. Richardson, E., Marone, C.: Effects of normal stress vibrations on frictional healing. J. Geophys. Res. **104**(B12), 28,859 (1999). doi:10.1029/1999jb900320
37. Scott, D.R., Marone, C.J., Sammis, C.G.: The apparent friction of granular fault gouge in sheared layers. J. Geophys. Res.: Solid Earth (1978–2012) **99**(B4), 7231–7246 (1994)